

Evidence for Single-gap Superconductivity in $\text{Mg}(\text{B}_{1-x}\text{C}_x)_2$ Single Crystals with $x = 0.132$ from Point-Contact Spectroscopy

R.S. Gonnelli,^{1,2} D. Daghero,^{1,2} A. Calzolari,¹ G.A. Ummarino,^{1,2} Valeria Dellarocca,¹ V.A. Stepanov,³ S.M. Kazakov,⁴ J. Jun,⁴ and J. Karpinski⁴

¹*Dipartimento di Fisica and INFM, Politecnico di Torino, 10129 Torino, Italy*

²*INFM - LAMIA, Corso Perrone 24, 16152 Genova, Italy*

³*P.N. Lebedev Physical Institute, Russian Academy of Sciences, 119991 Moscow, Russia*

⁴*Solid State Physics Laboratory, ETH, CH-8093 Zurich, Switzerland*

We report the results of the first directional point-contact measurements in $\text{Mg}(\text{B}_{1-x}\text{C}_x)_2$ single crystals with $0.047 \leq x \leq 0.132$. The two-gap superconductivity typical of MgB_2 persists up to $x = 0.105$. In this region, the values of the gaps Δ_σ and Δ_π were determined by fitting the Andreev-reflection conductance curves with a two-band Blonder-Tinkham-Klapwijk (BTK) model, and confirmed by the single-band BTK fit of the σ - and π -band conductances, separated by means of a magnetic field. At $x = 0.132$, when $T_c = 19$ K, we clearly observed for the first time the merging of the two gaps into one of amplitude $\Delta \simeq 3$ meV.

PACS numbers: 74.50.+r, 74.45.+c, 74.70.Ad

In the last three years, the great experimental and theoretical efforts of the scientific community have led to a clarification of most features of the intermetallic superconductor MgB_2 . These features are mainly related to the presence of two band systems (σ and π) and of the relevant gaps [1, 2]. Point-contact spectroscopy (PCS) has proved particularly useful in measuring both the σ - and π -band gaps at the same time [3, 4] and determining the temperature dependency of these gaps with great accuracy [4]. Very soon after the discovery of superconductivity in MgB_2 , substitutions of Al for Mg and of C for B were tried, in order to introduce impurities in the compound and modify its superconducting properties [5]. In particular, nearly single-phase $\text{Mg}(\text{B}_{1-x}\text{C}_x)_2$ polycrystals with $x \simeq 0.1$ were obtained by starting from Mg and B_4C [6, 7], which showed a linear dependence of the cell parameter a on the C concentration [7]. More recently, C-substituted MgB_2 single crystals were grown and many of their structural, superconducting and transport properties were measured [8, 9]. The first STM and PCS measurements on polycrystalline $\text{Mg}(\text{B}_{1-x}\text{C}_x)_2$ have shown the persistence of the two gaps up to $x = 0.1$ [10, 11, 12]. Up to now, the predicted achievement of single-gap superconductivity at a very high impurity level has never been observed.

This Letter presents the results of PCS measurements in $\text{Mg}(\text{B}_{1-x}\text{C}_x)_2$ single crystals with $0.047 \leq x \leq 0.132$, in the presence of magnetic fields up to 9 T either parallel or perpendicular to the c axis. These measurements gave us the dependence of the two gaps (Δ_π and Δ_σ) on the carbon content x and showed that, up to $x \simeq 0.10$, the two-gap superconductivity typical of unsubstituted MgB_2 is retained. At $x = 0.132$, we clearly and reproducibly observed for the first time the merging of Δ_π and Δ_σ into a single gap $\Delta = 3.2 \pm 0.9$ meV which shows a ratio $2\Delta/k_B T_c$ very close to the standard BCS value.

The high-quality $\text{Mg}(\text{B}_{1-x}\text{C}_x)_2$ single crystals were

grown at ETH (Zurich) with the same high-pressure technique adopted for unsubstituted MgB_2 [9], and by using either graphite powder or silicon carbide as a carbon source. Details on the structural and superconducting properties of these crystals can be found in a recent paper [9]. The 8 different carbon contents of our crystals were estimated from the lattice parameter a , assuming its linear dependence on x [7]. The resulting x values range between $x = 0.047$ and $x = 0.132$, corresponding to bulk critical temperatures between 35 K and 19 K.

We performed PCS measurements with the current mainly injected along the ab -planes of the crystal, since in unsubstituted MgB_2 this is the most favourable configuration for the contemporaneous measurement of both gaps [2, 4]. Hence, we select crystals with sharp edges and flat side surfaces, that unfortunately were not bigger than $0.5 \times 0.4 \times 0.08$ mm³. The point contacts were thus made on the narrow side of the crystals by using a small ($\varnothing \lesssim 50$ μm) spot of Ag conductive paint. With respect to the standard PCS technique – where contacts are made by pressing a metallic tip against the sample – this “soft” technique [4, 13] yields greater contact stability under thermal cycling and greater reproducibility of the conductance curves. By applying short current or voltage pulses to the junctions, we were able to tune their characteristics and achieve in most cases a normal-state resistance between 50 and 300 Ω . Since the in-plane mean free path in these single crystals ranges from $\ell \simeq 17.5$ nm to $\ell \simeq 13$ nm for x between 0.05 and 0.095 [9], these junctions result in the ballistic regime. The probable formation of parallel micro-junctions in the Ag-spot region explains the few cases where ballistic conduction, with no heating effects, is observed in low-resistance contacts.

Fig.1 reports some experimental conductance curves (dI/dV vs. V) of point contacts on $\text{Mg}(\text{B}_{1-x}\text{C}_x)_2$ crystals with different C contents (symbols). The curves are normalized to the normal-state conductance as explained

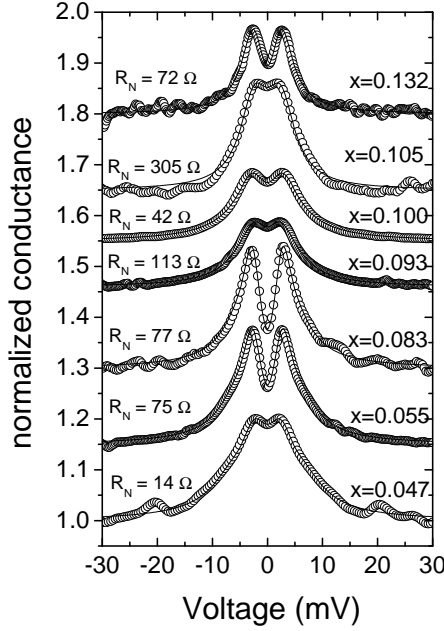


FIG. 1: Experimental normalized conductance curves of different ab -plane junctions in $\text{Mg}(\text{B}_{1-x}\text{C}_x)_2$ crystals with $0.047 \leq x \leq 0.132$ (open circles) and their two-band or single-band BTK fits (solid lines). The curves are vertically shifted for clarity and the corresponding values of the fitting parameters are shown in Table 1.

in Ref. [4]. As already shown by PCS in $\text{Mg}(\text{B}_{1-x}\text{C}_x)_2$ polycrystals [12], when $x \geq 0.047$ the experimental curves do not show the clear four-peaks structure typical of ab -plane contacts on unsubstituted MgB_2 [4]. In this situation, the proof of the presence of the σ -band gap and the determination of its value require a fitting procedure with the two-band BTK model [3, 4, 11, 12, 13] and/or the selective suppression of the π -band contribution to the conductance, for example by applying a suitable magnetic field [4, 13]. In the following we will present and discuss both these approaches.

First of all, let us discuss the fit of the zero-field conductance curves reported in Fig.1. In the two-band BTK model the normalized conductance of a point contact is given by $\sigma = (1 - w_\pi)\sigma_\sigma + w_\pi\sigma_\pi$ where σ_σ and σ_π are the partial σ - and π -band conductances, respectively, and w_π is the weight of the π band contribution. Each conductance depends on 3 parameters: the gap amplitude (Δ_σ or Δ_π), the potential barrier coefficient (Z_σ or Z_π) and the lifetime broadening parameter (Γ_σ or Γ_π). Thus, the total number of parameters in the model is 7. In unsubstituted MgB_2 , values of w_π ranging from 0.66 to 0.99 (depending on the angle made by the injected current with respect to the ab plane) were predicted [2] and very well confirmed by directional PCS [4]. In the absence of a similar prediction for the C-substituted compound, we conservatively used values of w_π between 0.66 and 0.8 in all the fits of our PCS curves.

The fitting procedure with the two-band BTK model

works very well for any x between 0.047 and 0.105. As shown in Fig.1, the agreement between experimental data (symbols) and fitting curves (lines) is very good. The best-fitting values of the parameters are listed in Table I. In the crystals with the highest C content, i.e. $x = 0.132$, the two-band BTK fit requires gap values very close to each other and, practically, interchangeable (in the sense that their error bars largely overlap). Thus, we tried a fit with the standard, single-band BTK model, and found out that it works even better than the two-band one. As a matter of fact, the solid line superimposed to the conductance curve at $x = 0.132$ in Fig.1 is obtained with only one gap of amplitude $\Delta = 2.8 \pm 0.2$ meV.

The reliability of the determination of Δ_σ and Δ_π by means of a seven-parameter fit may be questioned. Thus, we tried to apply here the same procedure that, in unsubstituted MgB_2 , yielded the most accurate determination of the temperature dependence of the gaps [4]. This procedure consists in separating the partial σ and π -band contributions to the total conductance, σ_σ and σ_π , by means of a suitable magnetic field, and in fitting each of them with the standard, three-parameter BTK model. A detailed discussion of the correctness and applicability of the BTK fit of Andreev reflection curves in the presence of magnetic fields is given in Ref. 13.

Fig.2 shows how this works in crystals with $x = 0.055$ (a) and $x = 0.100$ (b). In both panels, the zero-field conductance σ_0 (circles) is compared to the relevant two-band BTK fit (solid line). Diamonds represent instead the conductance σ_{B^*} measured in a magnetic field B^* (making an angle $\varphi = 90 \pm 2^\circ$ with the ab planes) that completely removes any structure related to the π -band gap [20]. For $x = 0.055$ this field is $B^* \simeq 2$ T, while for $x = 0.100$ it is $B^* = 1$ T, as in unsubstituted MgB_2 . Incidentally, this indicates that B^* has a maximum somewhere between $x = 0$ and $x = 0.100$, like the critical field [14, 15] and the irreversibility field [16]. σ_{B^*} contains only the σ -band contribution to the conductance and can thus be fitted by taking $\sigma_\pi = 1$ in the two-band BTK model. Since w_π is reasonably field-independent, only Δ_σ , Γ_σ and Z_σ remain as adjustable parameters. Finally, the difference $\sigma_{\text{diff}} = \sigma_0 - \sigma_{B^*} + 1$ (triangles) contains only

x	Δ_σ	Δ_π	Z_σ	Z_π	Γ_σ	Γ_π	w_π
0.047	7.0	3.2	0.5	0.34	3.15	1.6	0.66
0.055	6.6	3.0	0.48	0.52	2.5	1.1	0.75
0.083	5.8	2.99	0.5	0.57	2.6	0.91	0.7
0.093	4.3	2.8	0.56	0.38	3.2	2.0	0.7
0.10	4.9	3.28	0.53	0.42	4.55	2.07	0.69
0.105	4.25	3.2	0.57	0.33	2.55	1.62	0.80
0.132	2.8	-	0.52	-	1.50	-	0

TABLE I: Parameters of the best-fit curves of Fig.1 (solid lines)

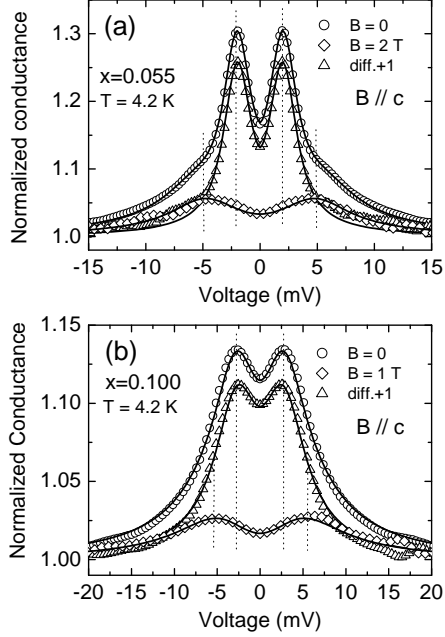


FIG. 2: (a) Normalized conductance curves of a *ab*-plane contact in a crystal with $x = 0.055$, at $B=0$ (circles) and $B=2$ T (diamonds). Triangles represent the difference of the previous two curves, shifted by 1. Solid lines: best-fitting curves given by the two-band (upper curve) or single-band (lower curves) BTK model. (b): same as in (a), but for a crystal with $x = 0.100$. Here the applied magnetic field is $B=1$ T. Vertical dashed lines roughly indicate the position of the conductance peaks.

the π -band conductance and can thus be fitted by taking $\sigma_\sigma = 1$ in the two-band BTK model [4].

The separate fit of σ_σ and σ_π gives the following results: (a) $\Delta_\sigma=5.45$ meV, $Z_\sigma=0.475$, $\Gamma_\sigma=2.4$ meV and $\Delta_\pi=2.30$ meV, $Z_\pi=0.488$, $\Gamma_\pi=0.485$ meV; (b) $\Delta_\sigma=4.9$ meV, $Z_\sigma=0.525$, $\Gamma_\sigma=4.55$ meV and $\Delta_\pi=3.28$ meV, $Z_\pi=0.42$, $\Gamma_\pi=2.07$ meV. In the case of $x = 0.055$, a slight reduction in Δ_σ is present with respect to the two-band fit (that gave $\Delta_\sigma=6.05$ meV and $\Delta_\pi=2.35$ meV), possibly because $B^*=2$ T is already comparable to $B_{c2}^{\parallel c}=8$ T [9] (in any case, these values are well compatible with each other within the error bars). For the case of $x = 0.100$, the parameters coincide with those reported in Table I. Similar agreement was found for any C content up to $x = 0.105$, and in all the junctions we studied, showing that this procedure has a high level of internal consistency and gives precise and reliable results, as in unsubstituted MgB_2 [4].

In the crystals with highest C content, $x = 0.132$, the same procedure gives quite different results and further confirms the presence of a single gap. Fig.3 reports the conductance curves of two different point contacts, in zero field (circles) and in the presence of a field of 6 T (diamonds) and 9 T (triangles), applied parallel to the *ab* plane (a) or to the *c* axis (b). In both cases, the strong reduction in the height of the curves indicates a strong

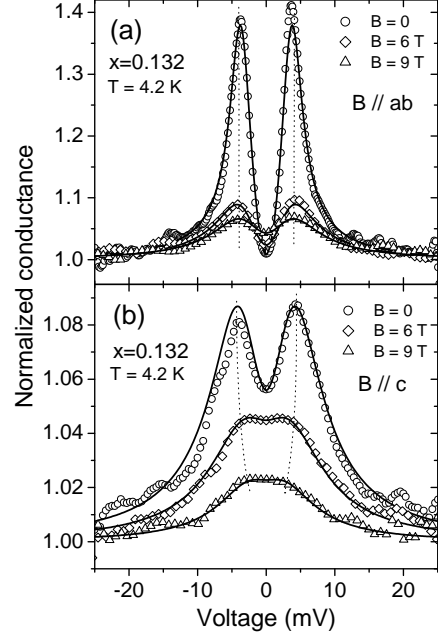


FIG. 3: Normalized conductance curves of two point contacts on a crystal with $x = 0.132$, in zero field (circles), and in the presence of a field of 6 T (diamonds) and 9 T (triangles). The magnetic field is parallel to the *ab* plane in (a) and parallel to the *c* axis in (b). Dashed lines roughly indicate the position of the conductance peaks. Solid lines are the single-band BTK best-fitting curves. Increasing the field from 0 to 9 T, the parameters vary as follows: $\Delta = 4.0 \rightarrow 3.5$ meV, $\Gamma = 0.8 \rightarrow 3.8$ meV, $Z = 0.60 \rightarrow 0.53$ for panel (a); $\Delta = 4.0 \rightarrow 2.0$ meV, $\Gamma = 3.6 \rightarrow 4.6$ meV, $Z = 0.52 \rightarrow 0.42$ for panel (b).

field-induced pair breaking. However, contrary to what happens at lower C contents, there is no clear shift of the conductance maxima towards higher energy (that is the hallmark of the suppression of the π -band contribution at $B = B^*$). Rather, the peaks approximately remain in the same position if $\mathbf{B} \parallel ab$, and shrink if $\mathbf{B} \parallel c$, as expected for an anisotropic single-gap superconductor with $B_{c2}^{\parallel ab} > B_{c2}^{\parallel c} > 9$ T. Indeed, all the curves can be fitted very well by the single-band BTK model, with a reasonable field-induced reduction of the gap. The best-fitting curves are reported in Fig.3 (solid lines), whose caption reports the relevant parameters.

The dependence of the gaps on the carbon content and on the bulk critical temperature of the crystals (determined by DC magnetization and AC susceptibility) is reported in Fig. 4 (a) and (b), respectively. Each point results from an average of various gap values (usually 4-8) obtained in different contacts by means of either a two-band or a single-band BTK fit. Hence, error bars indicate the maximum spread of measured values, and give an idea of the good reproducibility of our results. The value of the single gap at $x = 0.132$, $\Delta = 3.2 \pm 0.9$ meV, and the bulk $T_c = 19$ K, give a gap ratio $2\Delta/k_B T_c \sim 3.9$ close to the BCS value. The large uncertainty on Δ might arise

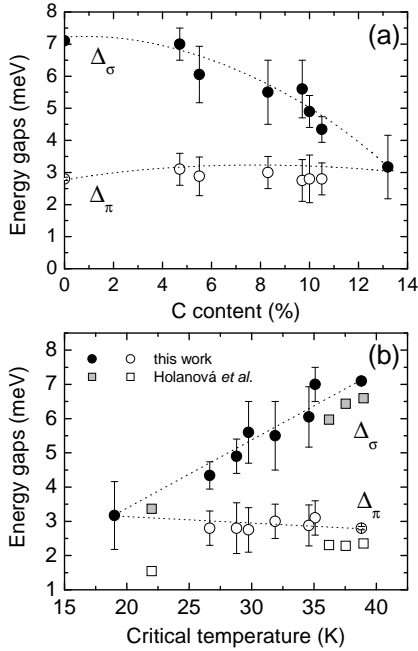


FIG. 4: Gap amplitudes, Δ_σ and Δ_π , as a function of the C content x (a) and of the bulk critical temperature T_c (b). In the latter case, data from PCS in polycrystals [12] are reported for comparison. Dotted lines are guides to the eye.

from inhomogeneities in the carbon content on a scale comparable to ξ [9]. However, note that *all* the curves at $x = 0.132$ were best-fitted by a single gap BTK model. In the whole range of C contents and critical temperatures, the gaps show a very regular and smooth trend. In Fig.4(b), our gap values are compared to data from PCS in polycrystals by Holánová et al. [12]. Apart from a small systematic shift, their $\Delta_\sigma(T)$ curve is in good agreement with our results in the whole doping range, while their value of Δ_π at $x = 0.10$ ($T_c = 22$ K), is much smaller than ours. We suggest that this disagreement may arise from the different nature of the samples.

The decrease in Δ_σ and the slight increase in Δ_π shown in Fig.4 seem to be compatible with an increase in *interband* scattering, as predicted by the two-band model. However, carbon substitution does not alter the local point symmetry of the lattice and therefore it should not lead to an increase in interband scattering [17]. Other effects, such as the changes in the electronic structure due to electron doping [18] and the hardening and narrowing of the E_{2g} phonon mode (that, in turn, indicate a reduction in the electron-phonon coupling) [14] have indeed been shown to play a major role, e.g., in determining the dependence of T_c on the C content. By taking into account analogous effects due to Al substitution, a behavior of the gaps qualitatively similar to that of Fig.4(a) was predicted within the two-band Eliashberg theory [19]. It is thus possible that, with suitable input from experiments and first-principle calculations,

this theory can properly reproduce also the observed $\Delta_\sigma(x)$ and $\Delta_\pi(x)$ curves in $\text{Mg}(\text{B}_{1-x}\text{C}_x)_2$ single crystals. Finally, the evidence here obtained of the achievement of single-gap superconductivity at $x = 0.132$, accompanied by an anisotropic bandstructure (suggested by the anisotropic magnetic properties, see Fig.3) is compatible with the extrapolation at $x > 0.10$ of recent measurements of B_{c2} and Hall effect carried out in single crystals up to $x = 0.10$ [14].

In conclusion, we have presented the results of the first directional point-contact measurements in $\text{Mg}(\text{B}_{1-x}\text{C}_x)_2$ single crystals with $0.047 \leq x \leq 0.132$, that allowed us to obtain the dependence of Δ_σ and Δ_π on the carbon content x . This dependence was confirmed by applying to the junctions a suitable magnetic field B^* able to remove the contribution of the π -band gap to the total conductance, thus allowing the separate determination of the gaps via a single-band BTK fit. Up to $x \sim 0.10$, the two-gap nature of superconductivity characteristic of unsubstituted MgB_2 is retained. At $x = 0.132$ we clearly and reproducibly observed for the first time the merging of the two gaps into a single gap $\Delta \simeq 3$ meV with a gap ratio $2\Delta/k_B T_c$ close to the standard BCS value and a critical field greater than 9 T.

This work was done within the Project PRA “UM-BRA” of INFM and the INTAS Project n.01-0617. V.A.S. acknowledges the support from RFBR (projects n. 04-02-1726 and 02-02-17133) and the Ministry of Science and Technologies of the Russian Federation (contract n. 40.012.1.1.1357).

-
- [1] A.Y. Liu, I.I. Mazin, and J. Kortus, Phys. Rev. Lett. **87**, 87005 (2001).
 - [2] A. Brinkman *et al.*, Phys. Rev. B **65**, 180517(R) (2001).
 - [3] P. Szabó *et al.*, Phys. Rev. Lett. **87**, 137005 (2001).
 - [4] R.S. Gonnelli *et al.*, Phys. Rev. Lett. **89**, 247004 (2002).
 - [5] R.J. Cava *et al.*, Physica C **385**, 8 (2003).
 - [6] R.A. Ribeiro *et al.*, Physica C **384**, 227 (2003).
 - [7] M. Avdeev *et al.*, Physica C **387**, 301 (2003).
 - [8] S. Lee *et al.*, Physica C **397**, 7 (2003).
 - [9] S.M. Kazakov *et al.*, preprint cond-mat/0405060.
 - [10] Schmidt *et al.*, Phys. Rev. B **68**, 060508 (2003).
 - [11] P. Samuely *et al.*, Phys. Rev. B **68**, 020505(R) (2003).
 - [12] Z. Holánová *et al.*, preprint cond-mat/0404096.
 - [13] R.S. Gonnelli *et al.*, Phys. Rev. B **69**, 100504(R) (2004).
 - [14] T. Masui, S. Lee, S. Tajima, preprint cond-mat/0312458.
 - [15] R.H.T. Wilke *et al.*, Phys. Rev. Lett. **92**, 217003 (2004).
 - [16] E. Ohmichi *et al.*, preprint cond-mat/0312348.
 - [17] S.C. Erwin and I.I. Mazin, Phys. Rev. B **68**, 132505 (2003).
 - [18] P. P. Singh, preprint cond-mat/0304436.
 - [19] G.A. Ummarino *et al.*, preprint cond-mat/0310284.
 - [20] We obtained similar results in the $\mathbf{B} \parallel ab$ configuration. Actually, the complex field effects on the conductance curves and their temperature dependence will be discussed in a forthcoming paper.